Bull. Mater. Sci., Vol. 38, No. 7, December 2015, pp. 1867–1873. © Indian Academy of Sciences.

Luminescent properties of red-light-emitting phosphors $CaWO_4 : Eu^{3+}$, Li^+ for near UV LED

F B XIONG*, H F LIN, L J WANG, H X SHEN, Y P WANG and W Z ZHU
Department of Optoelectronics, Xiamen University of Technology, Xiamen, Fujian 361024, China

MS received 20 August 2014; accepted 9 July 2015

Abstract. **A series of red phosphors $Ca_{1-2x}WO_4 : xEu^{3+}, xLi^+$ ($x = 0.01$, 0.02, 0.04, 0.06, 0.12, 0.20 and 0.30) in pure phase were synthesized via high-temperature solid-state reaction and their luminescent properties were investigated. For comparison, the 6 mol% Eu^{3+}-doped $CaWO_4$ was also obtained and investigated. The crystal structures of these phosphors were characterized by powder X-ray diffraction, and the luminescent properties of Eu^{3+}-, Li^+-codoped $CaWO_4$ were investigated by diffuse reflectance spectra, photoluminescence emission spectra, photoluminescence excitation spectra, and the Commission International de L' Eclairage (CIE) chromaticity indexes. These spectra illustrated that Eu^{3+}-, Li^+-codoped $CaWO_4$ phosphors could effectively be excited by a 270 nm ultraviolet (UV) or 394 nm near UV chip, and exhibit red emission originated from the $^5D_0 \rightarrow {}^7F_J$ ($J = 1$ and 2) transitions of Eu^{3+}. The fluorescent intensities of red emission band centred at 610 nm of 6 mol% Eu^{3+}-, Li^+-codoped $CaWO_4$ were about 1.27 times stronger than that of 6 mol% Eu^{3+}-doped $CaWO_4$ under 394 nm excitation. The 12 mol% doping concentration of Eu^{3+} ions in $CaWO_4$ is optimum when excited at 394 nm, while excited at 270 nm the sample with 6 mol% was the best one. The concentration quenching mechanism could be attributed to the dipole–dipole interaction between the Eu^{3+} ions. The CIE colour coordinates can be tuned from yellowish red to deep red with varying concentrations of Eu^{3+}. The present work suggests that Eu^{3+}-, Li^+-codoped $CaWO_4$ as red phosphors exhibit great potential application in the near UV excited white-light-emitting diode.**

Keywords. **Luminescent properties; red phosphors; energy transfer; concentration quenching; white LEDs.**

1. Introduction

InGaN-based white-light-emitting diodes (WLEDs), which are regarded as the fourth generation of illumination technology, have attracted increasing attention for their application in display lighting sources and illuminating systems because of their several advantages, such as high efficiency, energy savings, long lifetime, and positive environmental effects.[1–3] There are two approaches for generating white light using LEDs. One is the combination of tri-colours RGB LED chips, but its disadvantage is high cost, different drive voltage, and different thermal properties and degradation. The other is to couple a blue or ultraviolet (UV) LED with various primary colours from different emitting phosphors.[4–6] The currently commercial WLEDs are mainly obtained by combining a 460 nm blue-emitting GaN chip with a yellow-emitting yttrium aluminium garnet (YAG)-doped Ce^{3+} phosphor because of simple fabrication and mature processing. However, due to lacking of a red component this type of WLED exhibits low colour rendering index and high correlated colour temperature.[7,8] Therefore, in order to obtain warm white-light emission and a high colour rendering index, red phosphor is added to the system, which results in favourable outputs.[9] Another option to generate warm white-light source is to use UV LED chips and tri-colour (RGB) phosphors. Therefore, high-performance blue, green and red phosphors suitable to be excited by UV LED light have attracted much attention in recent years.[10] Even though many phosphors for white LEDs are currently available, red phosphors still have problem associated with low brightness and chemical instability.[11,12]

Intensive studies have been carried out on Eu^{3+}-doped red phosphors,[13–16] because there is an intense red emission band (about 600 nm) via the $^5D_0 \rightarrow {}^7F_2$ transition of Eu^{3+} ions if the Eu^{3+} is located in a non-centrosymmetric lattice site. Molybdates and tungstates have been widely researched, owing to their broad and intense charge-transfer absorption band in the UV and near UV spectral region and their excellent thermal and chemical stability.[11,13] Some Eu^{3+}-activated tungstates with a Scheelite structure have been demonstrated to emit strong red light under the near UV excitation.[15] The Eu^{3+}-doped Y_2MoO_6 has been investigated as promising red phosphor.[16,17] It has been demonstrated that Eu^{3+}: $CaWO_4$ and Eu^{3+}: $PbWO_4$ nanocrystals can be obtained by hydrothermal treatment and the influence of synthesis temperature on the particle size and luminescent properties have been researched.[15,18] Luminescent properties and afterglow phenomenon of Eu^{3+} in MWO_4 (M = Ca, Sr and Ba)

*Author for correspondence (fbxiong@xmut.edu.cn)

matrix have been explored.[19] In recent times, Eu^{3+}-doped $SrWO_4$ phosphors with various concentrations synthesized by microwave radiation heating have been reported as red phosphors.[20]

The luminescent properties of Eu^{3+}-doped $CaWO_4$ have been intensively investigated in recent times.[21] However, it has been demonstrated that the alkali metal ion codoped into tungstate matrix would lead to drastically increase in the luminescence intensities of Eu^{3+} : Y_2MoO_6,[16] because these ions have low oxidation state and distinct ionic radii, and could be used to modify the local site symmetry of the Eu^{3+} containing materials. Considering that the ionic radii of Li^+ ion is the smallest one among the alkali metal ions, and Li^+ ion becomes easily interstitial atom when Ca^{2+} ions are substituted by the Eu^{3+} ions in Eu^{3+}-, Li^+-codoped $CaWO_4$, in this paper, Eu^{3+}-, Li^+-codoped $CaWO_4$ phosphors with various Eu^{3+} doping concentrations have been extensively investigated to explore high-efficiency red phosphors. We compared the characteristic Eu^{3+} emissions under different excitation wavelengths, optimized the Eu^{3+} dopant concentration, and figured out the mechanism of energy transfer between the Eu^{3+} ions.

2. Experimental

The phosphors $Ca_{1-2x}WO_4 : xEu^{3+}, xLi^+$ ($x = 0.01$, 0.02, 0.04, 0.06, 0.12, 0.20 and 0.30) and $Ca_{0.94}Eu_{0.06}WO_4$ were prepared by the solid-state reaction method at high temperature. Stoichiometric amount of starting materials including $CaCO_3$ (analytical reagent, AR), WO_3 (AR), Li_2CO_3 and Eu_2O_3 (99.99%) were weighed and thoroughly ground in an agate mortar for 20 min, then transferred to a corundum crucible and pre-sintered at 300°C for 2 h in a muffle furnace. The obtained powders were reground and calcined at 1000°C for 3 h in air. After being cooled to room temperature naturally, the final products were ground to powder for measurement.

The phase structure of all the above phosphors were recorded for using a Panalytical X'pert pro X-ray diffractometer with Cu Kα source ($\lambda = 0.15418$ nm) operating at 40 kV and 40 mA with the scan range from 10° to 90° at about 2 deg min^{-1} speed. Diffuse reflectance spectra were recorded using a Lambda 650S (Perkin Elmer Co.) spectrophotometer. $BaSO_4$ was used as a reference for 100% reflectance during the measurement. The photoluminescence (PL) and PL excitation (PLE) spectra were measured by a Cary Eclipse fluorescence spectrophotometer with a microsecond flash Xe lamp as the excitation source (Agilent Technologies Co.). To ensure the same measurement condition, the phosphors were tightly packed into a cavity in a quartz holder and the holder was placed in a fixed position in all experimental set-up, and the fluorescence from the phosphors was detected with the same excitation and emission slit widths in the spectrophotometer. For the comparison of the fluorescent spectra at different excitation wavelengths, the response of the monochromator and detector at different wavelengths were corrected using a standard lamp (calibrated in the National Institute of Metrology, China). The Commission International de L'Eclairage (CIE) 1931 chromaticity coordinates of all the phosphors were obtained by a HAAS-2000 colour analyser equipped with a CCD detector (Yuanfang, Hangzhou, China). All the measurements were carried out at room temperature.

3. Results and discussion

Figure 1 presents the X-ray diffraction (XRD) patterns of $Ca_{1-2x}WO_4 : xEu^{3+}, xLi^+$ ($x = 0.01$, 0.02, 0.04, 0.06, 0.12, 0.20 and 0.30) and $Ca_{0.94}Eu_{0.06}WO_4$ phosphors. It is obvious that the position and relative intensity of the diffraction peaks of all the samples are almost consistent with the Inorganic Crystal Structure Database (ICSD no. 77-2233) and no impurity phase is observed. Even for the 30 mol% Eu^{3+}-, Li^+-codoped $CaWO_4$ phosphor, there is no second phase detectable. It means that the Eu^{3+} ions can be effectively incorporated into the sites of Ca^{2+} ions and Li^+ ions will become interstitial atoms in $CaWO_4$ matrix, because of the identical ionic radius of Eu^{3+} (1.12 Å) and Ca^{2+} (1.12 Å) ions and the smaller ionic radius of Li^+ ions. The doping of Eu^{3+} and Li^+ ions do not change the crystal structure.[19] The XRD patterns of $Ca_{0.94}Eu_{0.06}WO_4$ also agree well with that of the ICSD no. 77-2233 and no second phase can be found. $CaWO_4$ is tetragonal crystal system with $I4_1/a$ symmetry, and the crystal parameters are $a = b = 0.52429$ nm, and $c = 1.13737$ nm.[22] The XRD results illustrate that the doping Eu^{3+} and Li^+ ions are introduced to the crystal lattice without obviously changing the crystal structure.

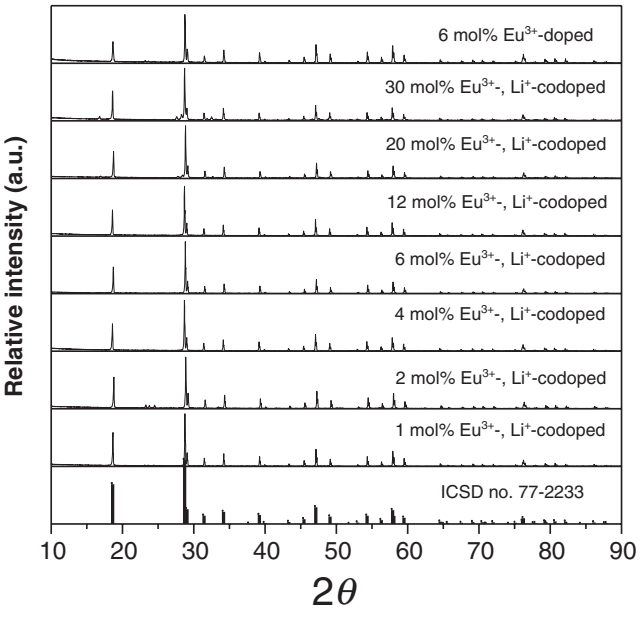

Figure 1. X-ray powder diffraction patterns of $Ca_{1-2x}WO_4 : xEu^{3+}, xLi^+$ ($x = 0.01$, 0.02, 0.04, 0.06, 0.12, 0.20 and 0.30) and $Ca_{0.94}Eu_{0.06}WO_4$ phosphors.

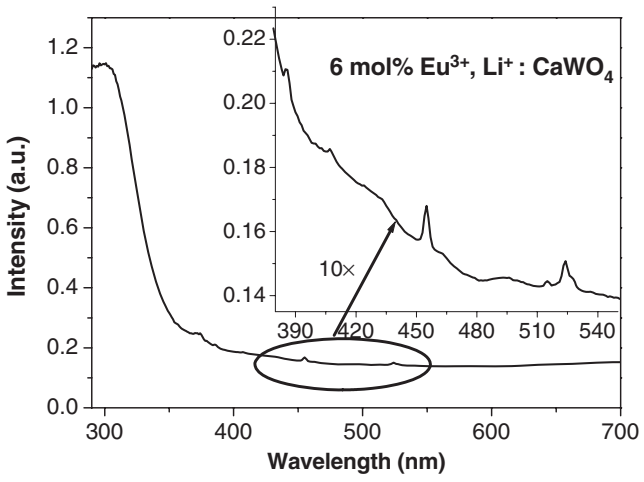

Figure 2. The ultraviolet–visible diffuse reflectance spectra of the 6 mol% Eu^{3+}, Li^+ : $CaWO_4$ phosphor and the inset shows enlargement of several absorption bands from the Eu^{3+} ions in $CaWO_4$.

The electronic transitions of the obtained phosphors were investigated by the ultraviolet–visible (UV–vis) reflectance spectra recorded by an integrating sphere. All reflectance spectra are similar and some typical spectrum of the $Ca_{0.88}WO_4 : 0.06Eu^{3+}, 0.06Li^+$ phosphor is shown in figure 2. The inset in this figure shows enlargement of the characteristic transitions of Eu^{3+} ion in the range of 380–540 nm. These weak lines located around 390, 460 and 530 nm can be assigned to the $^7F_0 \rightarrow {}^5L_6$, $^7F_0 \rightarrow {}^5D_2$ and $^7F_0 \rightarrow {}^5D_1$ electronic transitions of Eu^{3+} ion, respectively.[19,21] The intensities change dramatically in the range of 280–350 nm, which reveals that there is a strong board absorption band originating from the $CaWO_4$ host. On the basis of the reference assignment,[19,23] the broad absorption is due to the $^1A_1 \rightarrow {}^1T_2$ transition originated from the charge-transfer band of W^{6+}–O^- within the WO_4^{2-} group and the O–Eu charge transfer band from 2p orbit of O^{2-} to 4f orbit of Eu^{3+}. Based on the absorption band of the host in this figure, the optical bandgap value of $CaWO_4$ was estimated to be 4.13 eV.

Figure 3a shows the PL emission spectra of the 4 mol% Eu^{3+}-, Li^+-codoped $CaWO_4$ phosphors excited at 270 and 394 nm, corresponding to the host excitation and the Eu^{3+} excitation of the $^7F_0 \rightarrow {}^5L_6$ transition, respectively. Different from the Eu^{3+}-doped MWO_4 (M = Ca, Sr and Ba), in which the long-lasting luminescence were reported because the formation of cation vacancies resulting from the charge compensation patterns of $3Ca^{2+} = 2Eu^{3+}$+vacancy will act as the electron or hole trapped centres,[19,24] the afterglow phenomenon cannot be observed in Eu^{3+}-, Li^+-codoped $CaWO_4$. It means that the charge compensation pattern is Eu^{3+} substitution in Ca^{2+} sites via the path $2Ca^{2+} = Eu^{3+} + Li^+$, and no cation vacancies or oxygen defects is formatted in Eu^{3+}-, Li^+-codoped $CaWO_4$ phosphor.

For the PL spectra under the excitation wavelength of 270 nm, the emission originated from the tungstate group disappears completely, and the main emission bands are

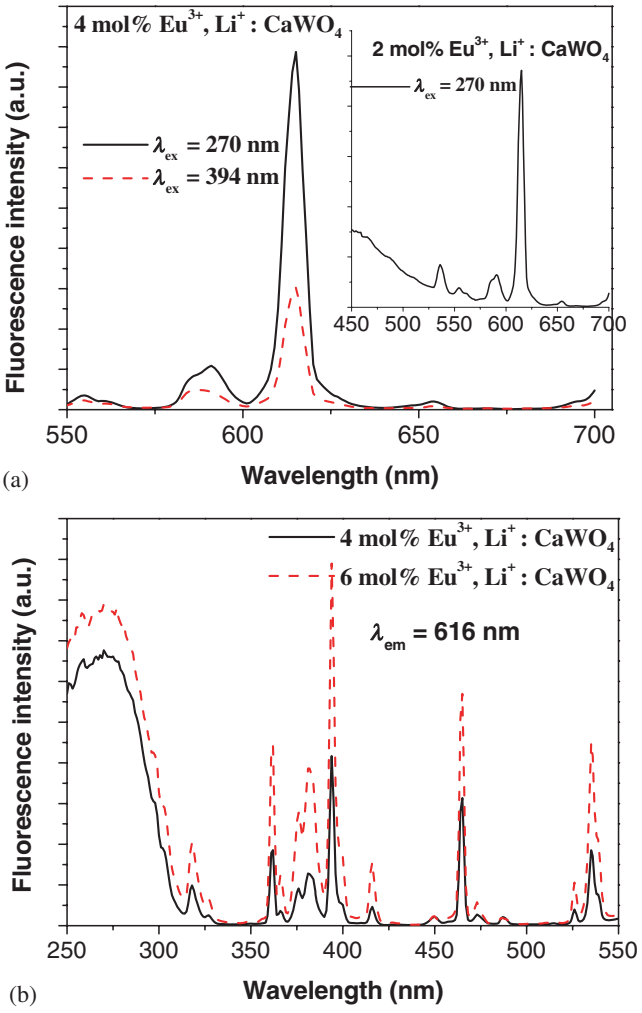

Figure 3. PL emission spectra (**a**) excited at 270 nm (black solid curves) and at 394 nm (red dash curves) of the 4 mol% Eu^{3+}, Li^+ : $CaWO_4$ phosphor, and PLE spectra and (**b**) monitored at 616 nm of the 4 mol% (black solid curves) and 6 mol% (red dash curves) Eu^{3+}, Li^+ : $CaWO_4$ phosphors.

attributed to the $^5D_0 \rightarrow {}^7F_J$ ($J = 1$ and 2) transitions of Eu^{3+}, corresponding to the typical 4f manifold transitions of Eu^{3+} ions. The emission spectra reveal two main emission bands which are at 591 nm ($^5D_0 \rightarrow {}^7F_1$) and 616 nm ($^5D_0 \rightarrow {}^7F_2$). The dominating emission band centred at 616 nm comes from the hypersensitive electronic dipole transition of $^5D_0 \rightarrow {}^7F_2$, and the weak emission band centred at 591 nm originates from the magnetic dipole transition of $^5D_0 \rightarrow {}^7F_1$. The PL emission spectra of the 4 mol% Eu^{3+}-, Li^+-codoped $CaWO_4$ phosphors excited at 394 nm are almost the same to that excited at 270 nm, except for the different emission intensities of two main bands. It is testified that the energy transfer process from the $CaWO_4$ host to the Eu^{3+} ions takes place. For further investigation of the energy transfer, the PL spectra of the 2 mol% Eu^{3+}-, Li^+-codoped samples excited at 270 nm were also recorded and are as shown in the inset in figure 3a. It can be found from the inset that a blue broad emission band originated

from the tungstate group appears; besides of the main characteristic emission bands from the Eu^{3+} ions in $CaWO_4$. It is demonstrated that the quenching of blue emission from the host is due to the energy transfer process, because in the $CaWO_4$ phosphors with the higher Eu^{3+} doping concentration, there are more Eu^{3+} activator and the quenching of blue host emission takes place. It is different from the previous report about the Eu^{3+}-doped $SrWO_4$, in which the blue emission band quenches due to the defects of crystal lattice.[20] One can find in figure 3a that for the 4 mol/% Eu^{3+}-, Li^+-codoped $CaWO_4$ phosphors, the luminescent emission intensities of the Eu^{3+} $^5D_0 \rightarrow {}^7F_2$ transition at 616 nm under the host excitation are much more stronger that that under the Eu^{3+} ions excitation at 394 nm, therefore for the Eu^{3+}-, Li^+-codoped $CaWO_4$ phosphors with low Eu^{3+} doping concentration, the host excitation is more efficient than the Eu^{3+} excitation.

The PLE spectra of the 4 and 6 mol% Eu^{3+}-, Li^+-codoped $CaWO_4$ phosphors were recorded and shown in figure 3b, monitored at 616 nm corresponding to the $^5D_0 \rightarrow {}^7F_2$ transition of Eu^{3+}. The broad strong absorption band centred at 294 nm in this figure belongs to the O–Eu charge transfer band from 2p orbit of O^{2-} to 4f orbit of Eu^{3+}, which is consistent with the results of UV–vis reflectance spectra (see figure 2). The appearance of charge transfer absorption band of the host in the excitation spectrum of Eu^{3+} ions verifies again that the energy transfer between the host and Eu^{3+} ions takes place. Several sharp absorption lines between 310 and 550 nm can be found in these figures, which correspond to the intraconfigurational $4f^6 \rightarrow 4f^6$ transitions of Eu^{3+} in $CaWO_4$ and the main absorption peak at 362, 394, 465 and 536 nm is assigned to the $^7F_0 \rightarrow {}^5L_8$, $^7F_0 \rightarrow {}^5L_6$, $^7F_0 \rightarrow {}^5D_2$ and $^7F_0 \rightarrow {}^5D_1$ transition, respectively. Because there are several strong absorption bands centred at 294, 394 and 465 nm for the Eu^{3+}-, Li^+-codoped $CaWO_4$ phosphors, these phosphors can efficiently be excited by the UV, near UV GaN-based or blue InGaN-based LED chips.

Some interesting results are worthy to note from figure 3b. Compared with the 4 mol% sample, for the 6 mol% phosphor the absorption intensities of the O–Eu charge transfer band from 2p orbit of O^{2-} to 4f orbit of Eu^{3+} centred at 294 nm are lower than that from the Eu^{3+} $^7F_0 \rightarrow {}^5L_6$ transition centred at 394 nm. It implies that for the Eu^{3+}, Li^+ : $CaWO_4$ phosphor with higher Eu^{3+} doping concentration, the excitation by the near UV GaN-based LED chip at 394 nm is more efficient than the host excitation at 270 nm. It also demonstrates that in the 6 mol% Eu^{3+}, Li^+ : $CaWO_4$ phosphors the energy from the charge-transfer band cannot completely sensitize the Eu^{3+} ions.

The PL emission spectra of 6 mol% Eu^{3+}-, Li^+-codoped and Eu^{3+}-doped $CaWO_4$ phosphors excited at 394 nm are shown in figure 4a. It is obvious that the PL emission spectra of both phosphors are similar and the PL intensities of red emission band centred at 615 nm from the 6 mol% Eu^{3+}-, Li^+-codoped $CaWO_4$ are about 1.27 times stronger than that of the 6 mol% Eu^{3+}-doped $CaWO_4$. It can be speculated that there are less cation vacancies or oxygen defects in the Eu^{3+}-, Li^+-codoped $CaWO_4$ compared with Eu^{3+}-doped

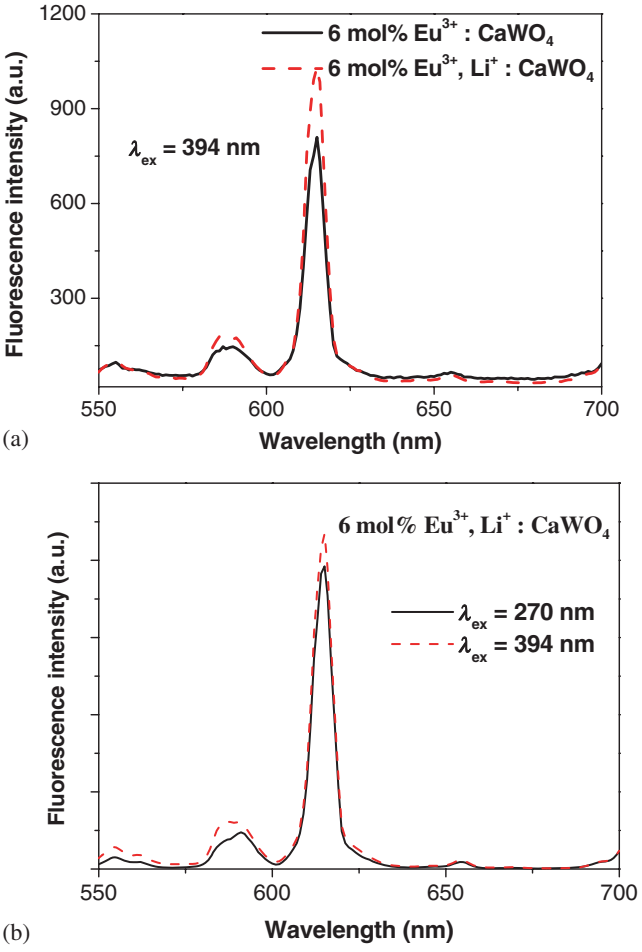

Figure 4. (**a**) PL emission spectra of 6 mol% Eu^{3+} : $CaWO_4$ (black solid curves) and 6 mol% and Eu^{3+}, Li^+ : $CaWO_4$ (red dash curves) phosphors, and (**b**) PL emission spectra excited at 270 nm (black solid curves) and 394 nm (red dash curves) of the 6 mol% Eu^{3+}, Li^+ : $CaWO_4$ phosphor.

$CaWO_4$. Therefore, the probabilities of nonradiative energy transfer between the excited Eu^{3+} ions and defect centres become small in Eu^{3+}-, Li^+-codoped $CaWO_4$, which has been demonstrated in the Eu^{3+}-, Li^+-codoped Y_2MoO_6 phosphors.[21]

To further investigate the energy transfer process, the PL spectra of the 6 mol% Eu^{3+}, Li^+ : $CaWO_4$ phosphors under the host excitation (excited at 270 nm) and the Eu^{3+} ions excitation (excited at 394 nm, corresponding to the $^7F_0 \rightarrow {}^5L_6$ transition of Eu^{3+}) are shown in figure 4b, respectively. Similar to the PL spectra of the 4 mol% Eu^{3+}-, Li^+-codoped sample shown in figure 3a, the blue emission band from the host is quenched and there are two main emission bands from the typical transitions of Eu^{3+} centred at 589 and 616 nm. The fluorescent intensities of the emission bands from the typical transitions of Eu^{3+} excited at 394 nm are stronger than that excited at 270 nm, which implies that the energy transfer between the Eu^{3+} and the host is inefficient for the samples with higher Eu^{3+}-doping concentration.

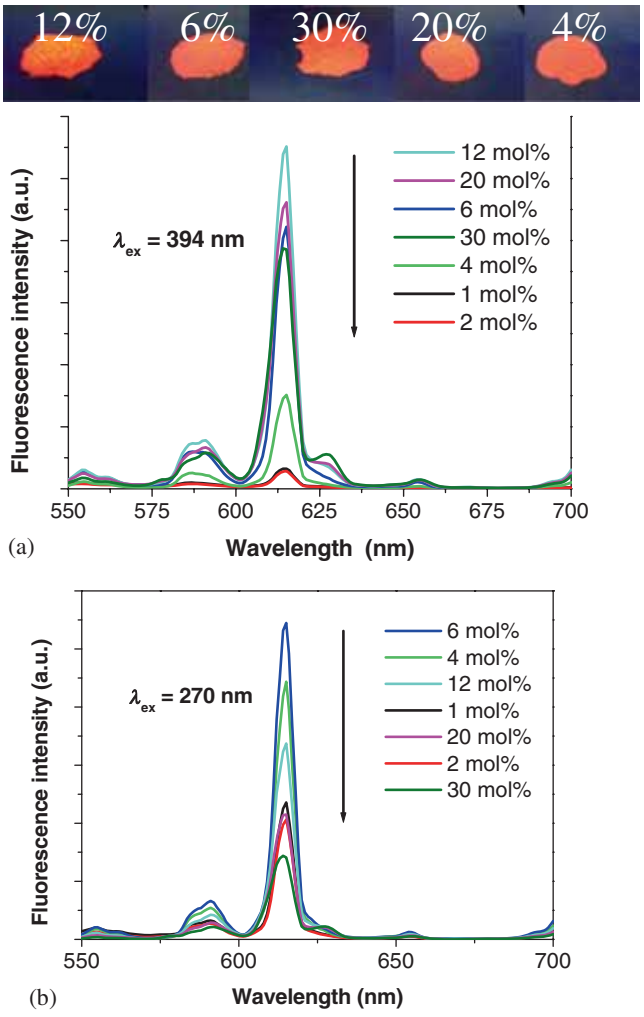

Figure 5. PL emission spectra excited at 394 nm (**a**) and PL emission spectra excited at 270 nm and (**b**) of the $Ca_{1-2x}WO_4 : xEu^{3+}$, xLi^+ (x = 0.01, 0.02, 0.04, 0.06, 0.12, 0.20 and 0.30), and the insets show images of the phosphors with various Eu^{3+} doping concentrations under an UV lamp emitting at 365 nm.

The PL emission spectra of $Ca_{1-2x}WO_4 : xEu^{3+}, xLi^+$ (x = 0.01, 0.02, 0.04, 0.06 0.012, 0.20 and 0.30) phosphors excited at 394 nm are shown in figure 5a. The PL spectra of those phosphors under the host excitation (excited at 270 nm) are presented in figure 5b. Similar to figure 4b, all those phosphors with different Eu^{3+} doping concentrations display the same emission spectra with different PL emission intensities, which certifies that the crystal structure of the $CaWO_4$ phosphors does not change with varying Eu^{3+} and Li^+ concentrations. Excited at 394 nm, two main emission bands from the characteristic transitions of Eu^{3+} ions are clearly observed in those phosphors with all doping concentration. It is observed that the fluorescence intensities of main emission bands increase with the increase in Eu^{3+} concentration. The fluorescent intensities of the emission bands centred at 589 and 616 nm reach maximum in the 12 mol% Eu^{3+}-, Li^+-codoped $CaWO_4$ phosphor. For the phosphors with higher Eu^{3+} concentration, there appears

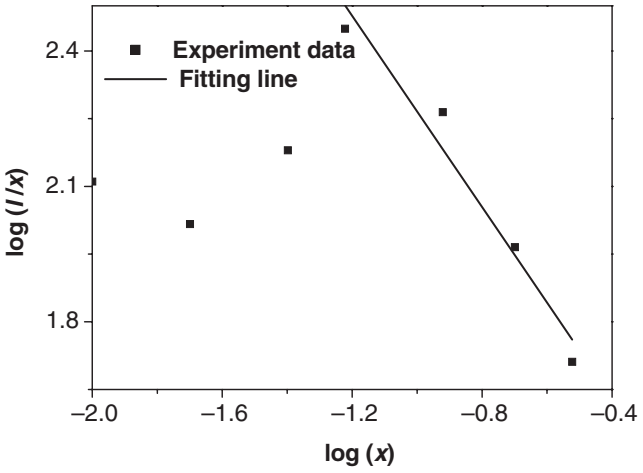

Figure 6. Plot of $\log(I/x)$ *vs.* $\log(x)$ for the $^5D_0 \rightarrow {}^7F_2$ transition of Eu^{3+} ions in $CaWO_4$ phosphor.

fluorescence concentration quenching. However, under the host excitation at 270 nm, the optimum Eu^{3+} doping concentration is about 6 mol%. One possible reason for the above observation is that, when the phosphors are excited at 270 nm, the energy transfer occurs between the host and the Eu^{3+} doping ions. However, excited at 394 nm, the Eu^{3+} ions are directly excited to the upper $^5L_6$ manifold. The energy transfer process will increase the possibility of concentration quenching due to some crystal lattice defects existing in the host. It is coincident with figures 3a and 4b, in which there are stronger fluorescence intensities in lower Eu^{3+} doping samples excited at 270 nm than that excited at 394 nm, for higher Eu^{3+} doping phosphors, the contrary situations happen. The insets of figure 5a show images of the $Ca_{1-2x}WO_4 : xEu^{3+}$, xLi^+ (x = 0.04, 0.06 0.012, 0.20 and 0.30) phosphors under an UV lamp emitting at 365 nm. As shown in the insets, it is obvious that the 12 mol% Eu^{3+}-doped phosphor emits the strongest red light in these phosphors, which is consistent with figure 5a. Therefore, among these phosphors obtained in this work, the 12 mol% Eu^{3+}-, Li^+-codoped $CaWO_4$ is the most potential red phosphors applied in the near UV excited WLEDs.

The concentration quenching in the Eu^{3+}-, Li^+-codoped $CaWO_4$ is due to energy transfer, and energy transfer processes from one Eu^{3+} to another can be described generally as multipolar interaction. The energy transfer mechanism between Eu^{3+} ions can be obtained by the equation according to the Van Uitert model.[25]

$$I/x = K\left[1 + \beta\,(x)^{Q/3}\right]^{-1}, \tag{1}$$

where I is the fluorescence emission intensity, x the activator concentration and Q the index of electric multipole, which is 6, 8 and 10 for electric dipole–dipole, electric dipole–quadrupole and electric quadrupole–quadrupole interaction, respectively; and K and β are constants for the same excitation condition for a given host crystal.

In figure 6 the fluorescence emission from the $^5D_0 \rightarrow {}^7F_2$ transition of Eu^{3+} ions in $CaWO_4$ phosphors excited at

Table 1. CIE coordinates of the $Ca_{1-2x}WO_4 : xEu^{3+}$, xLi^+ ($x = 0.04$, 0.06, 0.12, 0.20 and 0.30) phosphors excited at 394 nm.

Samples (x)	X coordinate	Y coordinate
0.30	0.604	0.394
0.20	0.613	0.386
0.12	0.637	0.363
0.06	0.644	0.350
0.04	0.655	0.344

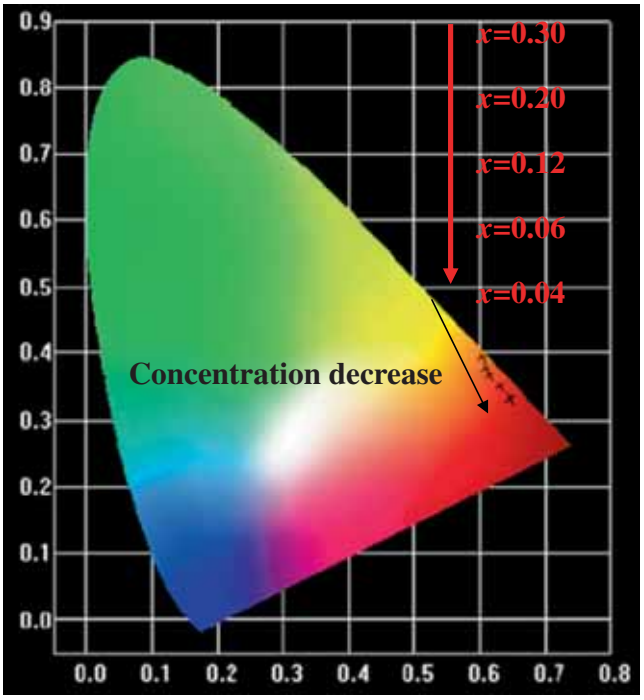

Figure 7. CIE diagram of $Ca_{1-2x}WO_4 : xEu^{3+}$, xLi^+ ($x = 0.04$, 0.06, 0.12, 0.20 and 0.30) phosphors excited at 394 nm.

394 nm is plotted as $\log(I/x)$ against $\log(x)$ plot. According to equation (1), using linearly fitting to deal with the experimental data when $x > 0.06$ in $Ca_{1-2x}WO_4 : xEu^{3+}$, xLi^+ ($x = 0.01$, 0.02, 0.04, 0.06, 0.012, 0.20 and 0.30), the slope parameter is obtained to be 1.68, which is approximately equal to 2, so the index of electric multipole energy transfer is 6. The result indicates that the dipole–dipole interaction is the major mechanism for concentration quenching of fluorescence emission in the Eu^{3+}-, Li^+-codoped $CaWO_4$ phosphors.

The CIE 1931 chromaticity coordinates of the Eu^{3+}-, Li^+-codoped $CaWO_4$ phosphors with various Eu^{3+} doping concentrations excited at 394 nm have been recorded by a colour analyser and listed in table 1. The CIE diagram of these phosphors is presented in figure 7 and the corresponding CIE coordinates are as shown in the inset of figure. It can be found that the chromaticity coordinates of these phosphors obtained in this study can be tuned from yellowish red ((0.604, 0.394), $x = 0.30$) to deep red ((0.655, 0.344), $x = 0.04$) with decreasing Eu^{3+} doping concentration in the $Ca_{1-2x}WO_4 : xEu^{3+}$, xLi^+ ($x = 0.04$, 0.06 0.012, 0.20 and 0.30) phosphors. It is demonstrated that the Eu^{3+}-, Li^+-codoped $CaWO_4$ phosphors with various Eu^{3+} concentrations can be defined as promising red emitting phosphors applied in the near UV-excited WLEDs.

4. Conclusions

In summary, a series of $Ca_{1-2x}WO_4 : xEu^{3+}$, xLi^+ ($x = 0.01$, 0.02, 0.04, 0.06, 0.012, 0.20 and 0.30) and $Ca_{0.94}Eu_{0.06}WO_4$ phosphors were successfully synthesized by traditional high-temperature solid-state reaction, and their PL properties were investigated in detail. Li^+ ions may serve as charge compensators and can reduce the defect centres in Eu^{3+}-, Li^+-codoped $CaWO_4$. The Eu^{3+}-, Li^+-codoped $CaWO_4$ can be efficiently excited by the near UV LED chips (394 nm) or UV LED chips (270 nm), and exhibit red emission originated from the $^5D_0 \rightarrow {}^7F_J$ ($J = 1$ and 2) transitions of Eu^{3+}. For these phosphors with the low Eu^{3+} doping concentration, the host excitation at 270 nm is more efficient. The critical quenching concentration of Eu^{3+} in the Eu^{3+}-, Li^+-codoped $CaWO_4$ is 12 and 6 mol%, when excited at 394 and 270 nm, respectively. One possible reason for different quenching concentrations is that the energy transfer process between the host and the Eu^{3+} ions is affected by the crystal lattice defects. The energy transfer mechanism between Eu^{3+} ions in $CaWO_4$ is dipole–dipole interaction. The colour coordinates can be tuned from yellowish red to deep red with the decrease in Eu^{3+} doping concentration in the Eu^{3+}-, Li^+-codoped $CaWO_4$. Therefore, it can be concluded that Eu^{3+}-, Li^+-codoped $CaWO_4$ phosphors are potential candidates as red phosphors for application in the UV or near UV-excited WLEDs.

Acknowledgements

This work has been supported by the Natural Science Foundation of China (Grant no. 11104234), the SRF for ROCS, SEM, Science Technology innovation project of Xiamen (3502Z20123044), and the S&T plan projects of Fujian Provincial Education Department (Grant nos JA12242 and JA12252).

References

1. Nishida N, Ban T and Kobayashi N 2003 *Appl. Phys. Lett.* **82** 3817
2. Schubert E F and Kim J K 2005 *Science* **308** 1274
3. Hashimoto T, Wu F, Speck J S and Nakamura S 2007 *Nat. Mater.* **6** 568
4. Zhang Z W, Song A J, Ma M Z, Zhang X Y, Yue Y and Liu R P 2014 *J. Alloys Compds.* **601** 231
5. Saradhi M P and Varadaraju U V 2006 *Chem. Mater.* **18** 5267

6. Zhou X and Wang X 2014 *Bull. Mater. Sci.* **62** 96
7. Wang J G, Jing X P, Yan C H and Lin J H 2005 *J. Electrochem. Soc.* **152** G186
8. Chao W-H, Wu R-J and Wu T-B 2010 *J. Alloys Compd.* **506** 98
9. Ju H, Wang L, Wang B, Ma Y, Wang H, Chen S and Tao X 2013 *Ceram. Int.* **39** 8001
10. Haque M M, Lee H I and Kim D K 2009 *J. Alloys Compd.* **481** 792
11. Tian L H, Yang P, Wu H and Li F Y 2010 *J. Lumin.* **130** 717
12. Tian L H and Mho S-I 2007 *J. Lumin.* **122–123** 99
13. Parchur A K, Ningthoujam R S, Rai S B, Okram G S, Singh R A, Tyagi M, Gadkari S C, Tewari R and Vatsa R K 2011 *Dalton Trans.* **40** 7595
14. Lu Z G, Chen L M, Tang Y G and Li Y D 2005 *J. Alloys Compd.* **387** L1
15. Wang X, Liu B and Yang Y 2014 *Opt. Laser Technol.* **58** 84
16. Jian H, Wu H and Tian L 2012 *J. Lumin.* **132** 1188
17. Han B, Zhang J, Wang Z, Liu Y and Shi H 2014 *J. Lumin.* **149** 150
18. Su Y G, Li L P and Li G S 2008 *Chem. Mater.* **20** 6060
19. Kang F W, Hu Y H, Chen L, Wang X J, Wu H Y and Mu Z F 2013 *J. Lumin.* **135** 113
20. Feng H, Yang Y and Wang X 2014 *Ceram. Int.* doi: 10.1016/j.ceramint.2014.01.129
21. Zhang Q, Meng Q and Sun W 2013 *Opt. Mater.* **35** 915
22. Hazen R M, Finger L W and Mariathasan J W E 1985 *J. Phys. Chem. Solids* **46** 253
23. Mikhailik V B, Kraus H, Miller G, Mykhaylyk M S and Wahl D 2005 *J. Appl. Phys.* **97** 083523
24. Fu J 2000 *Electrochem. Solid-State Lett.* **3** 350
25. Van Uitert L G 1967 *J. Electrochem. Soc.* **114** 1048